Optimal Shape Design of a Class of Permanent Magnet Motors in a Multiple-Objectives Context

Paolo Di Barba[*], Maria Evelina Mognaschi[*], Lidija Petkovska[**], Goga Cvetkovski[**]

** Dept. of Electrical, Computer and Biomedical Engineering,University of Pavia, Via Ferrata 5,27100 Pavia, Italy, {paolo.dibarba, eve.mognaschi}@unipv.it*

[**] Faculty of Electrical Engineering and IT, Ss Cyril&Methodius University, 1000 Skopje, North Macedonia {lidijap, gogacvet}@feit.ukim.edu.mk

Abstract

Design/methodology/approach: Two approaches are proposed in the paper: the All-Objectives (AO) and the Many-Objectives (MO) optimisation approach. The former is based on a single-objective optimization of a preference function i.e. a normalized weighted sum. In contrast, in the MO a multi-objective optimization algorithm is applied to the minimization of a weight-free preference function and simultaneously to a maximization of the distance of the current solution from the prototype. The optimizations are based on an equivalent circuit model of the Permanent Magnet (PM) motor, but the results are assessed by means of Finite Element Analyses (FEAs).

Purpose: The paper deals with the optimal shape design of a class of permanent magnet motors by minimizing multiple objectives according to an original interpretation of Pareto optimality. The proposed method solves a many-objective problems characterized by five objective functions and five design variables with evolution strategy algorithms, classically used for single- and multi-objective (two objective functions) optimization problems.

Findings: An extensive study of the solutions obtained by means of the different optimization approaches is provided by means of post-processing analyses. Both the approaches find non-dominated solutions with respect to the prototype that are substantially improving the initial solution. The points of strength along with the weakness points of each solution with respect to the prototype are analysed in depth.

Originality/value: Considering simultaneously five objective functions in an automated optimal design procedure is challenging. The proposed approach, based on a well-known and established optimization algorithm, but exploiting a new concept of degree of conflict, can lead to new results in the field of automated optimal design in a many-objective context.

Keywords: *Shape design, Permanent magnet motor, Stochastic algorithms, All-objective optimisation, Many-objective optimisation*

Paper Type: Research paper

1. INTRODUCTION

Permanent magnet (PM) motors working either as brushless DC motors (PMBLDC) or as synchronous AC motors (PMSM) are becoming much sought-after due to their superior performance characteristics, smooth control and higher energy efficiency. Recently, the topology of a permanent magnet motors is under reconsideration and new, attractive designs for improved performance motors with improved efficiency values are developing Pellegrino *et al.* (2016), Zhang *et al.* (2016) and Villani *et al.* (2018).

The motor performance depends on many factors which determine the electromagnetic properties and field distribution inside the motor domain. The main task of an electric motor designer is, for a given set of objective functions, to find the optimal shape design, Jabbari *et al.* (2010), getting the best possible motor performance at the least material usage, while satisfying given criteria and prescribed physical or technical limitations. In the literature there is plenty of contributions, which at a first glance could be categorized in two broad classes, namely: papers dealing with the magnetic analysis of a given motor comparing the effect of various materials and under several load conditions Najgebauer *et al.* (2019) and Przybylski *et al. (*2020), on the one hand, and papers focused on the automated optimal design of a class of motors, on the other hand Yan *et al.* (2019) and Putek *et al.* (2017).

As far as the latter are concerned, there is a remarkable tendency to simultaneously consider many objective criteria which are in mutual conflict, and so increasing the dimensionality of the objective space in a substantial way. It could be stated that algorithms based on the identification of the whole Pareto front are increasingly less effective in terms of selectivity when the objective space dimension is higher than 2 or 3.

In fact, many-objective problems – in contrast to multi-objective ones – originate a number of challenges to any optimisation algorithm, and so evolutionary ones are no exception. There are various reasons for that, like e.g.:

- the non-dominated solutions saturate most of the population slots; consequently, most solutions are indifferent according to Pareto-like optimality;
- implementing a diversity-preservation strategy is computationally expensive;
- the visualization of a large-dimensional front of non-dominated solutions is not trivial and makes it difficult the decision-making task and also the evaluation of algorithm performance.

A possible remedy is to revisit the concept of non-dominated solution: instead of following the classical definition in terms of solution dominance against all the objectives, in an equivalent way, one could think of best-compromise solutions like those exhibiting the least degree of conflict among all objectives. So, if a technique is devised for computing the degree of conflict of a solution, a search for least-conflict solutions driven by evolutionary computing can be implemented.

A contribution to bridge the gap, applied in the optimal shape design of a PM motor, is here proposed. The paper is organized as follows: a specific type of PM motor selected as the case study is presented, and the relevant optimal shape design problem is defined. Subsequently, two optimization approaches are described in a comparative way. Eventually, an in-depth discussion of optimization results is presented and concluding remarks follow.

2. THE CASE STUDY

Performance specifications and requirements for higher energy efficiency are vital for application of electrical machines. To improve motor performance is of great significance to energy sustainability and environment protection. This goal is achieved by shape design and optimization of electric motors. Besides the energy efficiency, there are many other specifications and/or requirements for design optimization of electrical machines, such as shaft torque, power density, motor volume and weight, materials, production cost, etc.

The proposed optimisation procedure in a many-objective context for shape design is applied on a permanent magnet synchronous motor (PMSM) representing the PMSM class. The drive can work in two typical operating regimes: (a) as a brushless DC permanent magnet (BLDCPM) motor, typically working as low inertia servomotor, with torque control 0-10 Nm and speed control 0-4000 rpm; (b) as a standard permanent magnet synchronous (PMSM) motor supplied from a three phase sinewave AC source, here taken as for *case study*.

In this regime the motor operates as standard PMSM with rated data: U_n = 42 V@50 Hz, I_n = 17.6 A, n_n = 1000 rpm, T_n = 10 Nm. The stator core lamination is with 36 slots; on the rotor surface are mounted 6 radially magnetized samarium-cobalt PMs, with remanence B_r = 0.95 T and with coercivity H_c = −720 kA/m. Three single-layer stator phase windings are Y- connected. In Figure 1 the cross-section of original motor lamination is depicted.

Due to manufacturing and motor assembly requirements, as seen in the figure, along the outside stator surface there are slots, notches and interlocks. On the other hand, as motor serves as a low-inertia servomotor – in order to reduce the rotor mass – on the rotor six holes in accordance with the position of permanent magnets are designed. Based on the numerical FEM simulations this complex original lamination geometry, without interfering the accuracy of the motor modelling and deteriorating the results, can be simplified, as presented in Figure 2.

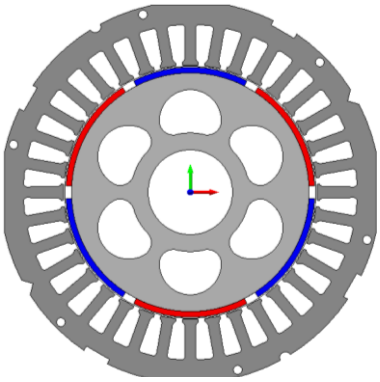

Figure 1: Original geometry of PMSM

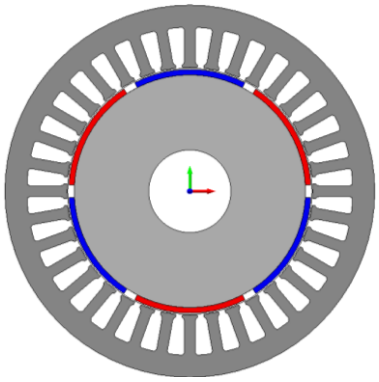

Figure 2: Simplified cross section of PMSM

The computational results for magnetic field distribution of the motor at no-load, presented for the original motor (a) and the studied motor (b) show similar features, foremost in the stator core, where no significant difference in the field properties can be noticed. Hence, when solving a design optimisation problem, the PMSM motor with simplified geometry will be considered as a *prototype motor*.

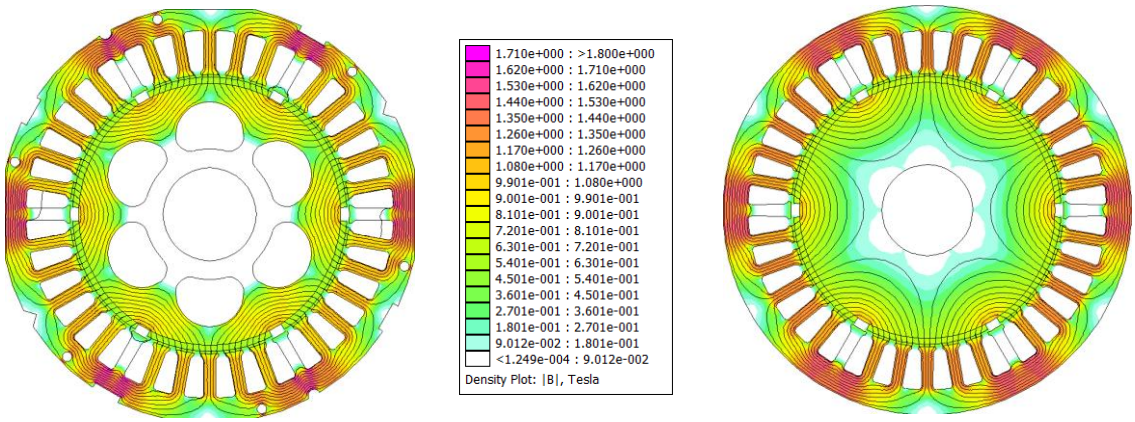

(a) Original motor *(b) Studied motor – a prototype*

Figure 3: Numerical experiment for geometry simplification of the PMSM

In order to reduce the computational cost, a circuit-like analytical model Cvetkovski *et al.* (2021), amenable to the theory of PMSM will be utilized for analysis during the optimization procedure, while the convergence geometry will be re-analysed with a finite-element model for assessing the optimisation results.

3. DESIGN OPTIMISATION PROBLEM

Design optimisation of electromagnetic devices has never been an easy task. Even more, the design optimization processes become more and more complex as several different engineering disciplines are involved, e.g. electromagnetics, structural mechanics, heat transfer, material science, etc. Usually the design of an electric machine has to satisfy rather conflicting objectives, such as high torque density, high motor efficiency or less loss, but at lower mass of active materials, or lower production costs.

In general, design optimisation problem of an electric motor is considered as a multi-objective or, more recently, a many-objective task while fulfilling various constraints, restrictions and physical or technical limitations. Design optimization of electric motors includes two main stages:

- Development of a mathematical model, by which the motor performance is described with a system of equations and the calculated parameters and characteristics are with the highest possible accuracy. The fidelity of the model is checked with initial design data of the prototype motor. Where available, the experimental data from the motor testing are also used.

- Once the equivalent circuit motor model has been proved as accurate enough, the shape optimization and optimal design for an improved motor performance is carried out.

The optimization problem can be cast as follows: starting from data for a prototype, find the motor geometry which simultaneously minimises a set of objective functions subject to the problem constraints. Selection of the objective functions is a user-defined problem, depending on the goals to be achieved. Assuming constant torque T_n, a motor designer can seek for maximum pull-out torque or minimum peak cogging torque. A good approach is to maximise efficiency, by minimisation of total loss. Aiming to reduce the size and weight of the motor, one possible objective function is to minimise the volume (D^2L), or to maximise torque volume density; the other approach is to minimise the weight of active materials: iron for cores, copper for windings and permanent magnets. Hence, proper selection of objective function(s) is of the greatest importance.

To illustrate a design optimisation problem solution, as well as application of the optimisation techniques that are proposed in this paper, for the studied permanent magnet motor PMSM, a constant rated shaft torque T_n and a constant rated rotor speed n_n are assumed. Then, in view of a multiple objective optimization, the following five single objective functions are selected, defining the **F**-space vector:

$$\mathrm{f}_1(\mathrm{x}) = P_{loss} \tag{1}$$

$$\mathrm{f}_2(\mathrm{x}) = \mathrm{m}_{tot} \tag{2}$$

$$\mathrm{f}_3(\mathrm{x}) = \eta \tag{3}$$

$$\mathrm{f}_4(\mathrm{x}) = D^2 L \tag{4}$$

$$\mathrm{f}_5(\mathrm{x}) = \frac{T_n}{V_m} \tag{5}$$

Where:

- The total losses $\mathrm{f}_1(\mathrm{x})$: $P_{loss} = P_{Cu} + P_{Fe} + P_{fw}$ to be minimised;
- The total active material mass $\mathrm{f}_2(\mathrm{x})$: $m_{tot} = m_{Cu} + m_{Fe} + m_{PM}$ to be minimised;
- The motor efficiency $\mathrm{f}_3(\mathrm{x})$: $\eta = [P_{2n}/(P_{2n} + P_{tot})]\cdot 100$ to be maximised;
- The motor design factor $\mathrm{f}_4(\mathrm{x}) = D^2L$ to be minimised; D is the inner diameter of the stator core and L is the axial length of the motor;
- The torque density $\mathrm{f}_5(\mathrm{x}) = T_n/V_m$, i.e. the shaft torque T_n per motor volume V_m, to be maximised.

Thus, the **F**-space for the selected objective functions is defined with:

$$\mathbf{F} = [\mathrm{f}_1, \mathrm{f}_2, \mathrm{f}_3, \mathrm{f}_4, \mathrm{f}_5] \tag{6}$$

while the general form of the initial space vector is:

$$\mathbf{F_0} = [\mathrm{f}_{01}, \mathrm{f}_{02}, \mathrm{f}_{03}, \mathrm{f}_{04}, \mathrm{f}_{05}] \tag{7}$$

Taking the values from the reference motor – a prototype PMSM, the initial space vector $\mathbf{F_0}$ becomes:

$$\mathbf{F_0} = [186.5\ (\mathrm{W}),\ 8.79\ (\mathrm{kg}),\ 84.89\ (\%),\ 7.29\cdot 10^{-4}\ (\mathrm{m}^3),\ 7.76\cdot 10^{3}\ (\mathrm{Nm/m}^3)] \tag{8}$$

The selection of design variables is another main task to be accomplished. Shape optimisation parameters are problem dependent and their selection is consistent with formulation and selection of the objective functions. By using them the mathematical model of the motor is fully described.

In this study the problem is characterized by a set of five independent design variables which are: the rotor core radius $R_R = \mathrm{x}_1$, the air gap length $g = \mathrm{x}_2$, the permanent magnet height $h_{PM} = \mathrm{x}_3$, the permanent magnet pole coverage $f_m = \mathrm{x}_4$ and the axial length of the motor $L = \mathrm{x}_5$, as depicted in Figure 4.

Hence, the **X**-space for the design variables is determined by the vector:

$$\mathbf{X} = [\mathrm{x}_1, \mathrm{x}_2, \mathrm{x}_3, \mathrm{x}_4, \mathrm{x}_5] \tag{9}$$

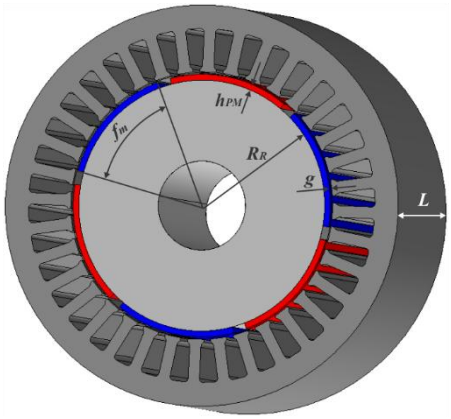

Figure 4: Visual presentation of independent design variables

In order to keep the motor frame and the shaft same as in the prototype, during the optimisation procedure the outer diameter of stator core and the inner diameter of rotor core are with fixed values. Thus, when the selected independent variables in radial direction (R_R, g, h_{PM}) are freely varied, the stator inner radius R, the slot height h_s and the stator yoke height h_Y – being the dependent variables – will be subject to corresponding changes; accordingly, the stator tooth width b_t will be also changed. To avoid saturation of the stator core, the maximum value for magnetic flux density in the yoke and teeth is prescribed.

Optimisation procedure is starting from the prototype values characterized by:

$$\mathbf{X_0} = [x_{01}, x_{02}, x_{03}, x_{04}, x_{05}] = [42\ (\text{mm}), 0.8\ (\text{mm}), 2\ (\text{mm}), 0.9, 90\ (\text{mm})] \tag{10}$$

The vector $\mathbf{X_0}$ is considered as initial solution. To assure a feasible optimal solution, the variation range of the design variables in the **X**-space is set $\pm\ 15\%$ of the prototype values. The only exception is the permanent magnet pole coverage, which is maximised with $f_m \leq 1$. Based on experience, it is considered the change interval ±15% from the reference values of the prototype motor is satisfactory enough.

4. OPTIMISATION APPROACHES

In the paper two approaches are considered: the All-Objectives (AO) and the Many-Objectives (MO) optimisation techniques. The idea behind the paper is *first* to exploit a single-objective optimization algorithm for minimising a suitable preference function, which takes into account all the separate defined single objective functions of the studied optimization problem. The chosen method is *EStra* – a lowest-order *E*volution *Stra*tegy – which has been proven to be well effective and high reliable, Di Barba *et al.* (2005).

4.1. ALL-Objectives Optimisation Context

To accomplish optimal shape design for the studied PMSM, in the paper a respective combination of all single objective functions f_1 – f_5, here called *All Objectives (AO) Optimisation* is used, Di Barba *et al.* (2009). Traditionally, the combined objective function F_{ALL} is defined as weighted sum of individual preference objectives. However, having in mind that the choice of individual weights is a bias, we suggest to use the linear combination of individual objective functions. Because of the different 'nature' of the five objective functions, their normalised values should be used:

$$\mathbf{F_{ALL}(x)} = \frac{\mathbf{f_1(x)}}{\mathbf{f_{01}}} + \frac{\mathbf{f_2(x)}}{\mathbf{f_{02}}} - \frac{\mathbf{f_3(x)}}{\mathbf{f_{03}}} + \frac{\mathbf{f_4(x)}}{\mathbf{f_{04}}} - \frac{\mathbf{f_5(x)}}{\mathbf{f_{05}}} \tag{11}$$

The AO context considers one preference function $F_{ALL}(x)$, eq. (11), which takes into account all the five objective functions, defined with eqs. (1) – (5), by means of a weighted sum, characterized by their unit weights. As explained before, the normalization and determination of the corresponding unit weights is done with respect to the prototype

values, eq. (8). Then, preference function is minimized by means of the EStra method, a lowest-order evolutionary algorithm, which has been proven to be effective and reliable.

4.2 Many-Objectives Optimisation Context Please check this heading and make improvements (if any)

In contrast to AO optimisation technique, the idea behind the *Many-Objective (MO) Optimisation* approach is to exploit another preference function, Di Barba *et al.* (2019), which takes into account all the objective functions of the optimization problem Di Barba *et al.* (2020), with no need of calculating a weighted sum. In the proposed MO method, the aim is to define a weight-free preference function $f_P(x)$: in view of this context, the key idea is the introduction of a degree of conflict among solutions, because in Pareto-like optimality the non-dominated solutions exhibit the lowest degree of conflict in the set of solutions.

Moreover, in order to increase the diversity in shape between the prototype and the optimal solution, the following function is defined:

$$g_2(x_{sol}) = \sqrt{\sum_{i=1}^{n_v} \left(\frac{x_{i,0} - x_{i,sol}}{x_{i,0}} \right)^2} \tag{12}$$

where x_{sol} is the design vector relevant to the current solution.

Hence, the main steps are:

- define a preference function, modelling the degree of conflict among objectives, whatever the number of objectives;
- minimise the preference function f_P and maximise function g_2 by means of a multi-objective evolution-strategy algorithm MO–EStra, Di Barba *et al.* (2005), i.e. a derivative-free and global-optimum oriented algorithm;
- identify a set of least-conflict solutions, approximating a Pareto-optimal set.

The core operation is to compute the degree of conflict between m≥2 objective functions (f_1, f_2,…,f_m) that are assumed to be simultaneously minimized. After sorting in the ascending order, the rank of a solution is defined as the sorting index of the relevant objective function values. The computation of the degree of conflict of a solution – called *score* – is based on the sorting indices of the objective functions. There are various techniques for computing the degrees of conflict; here, we propose a simple technique based, for each solution, on the sum of the ranks c_k with k=1, ….. m.

The flow-chart for the many-objective computing procedure is presented in Figure 5.

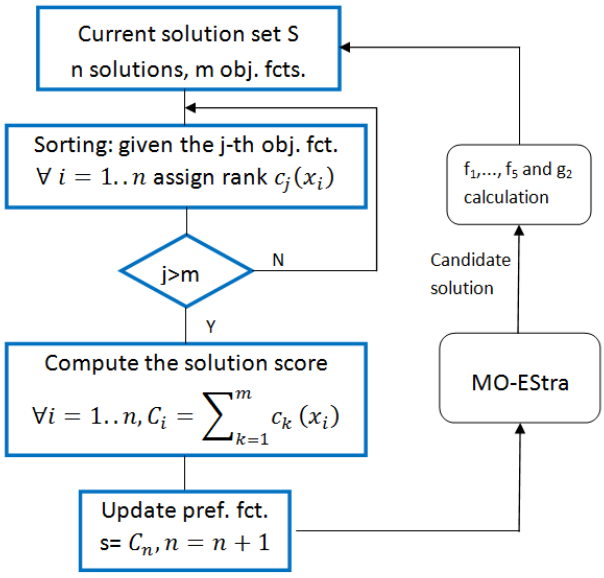

Figure 5: Flow-chart of the many-objective algorithm

In fact, every candidate solution is attributed the score as the sum of the partial scores, each of which is relevant to one objective function. Eventually, the goal is to simultaneously minimize the score s and maximize the function g_2 with respect to any x in the design space Ω. Whenever a new candidate solution is created by the algorithm, the set S is expanded by incorporating the (n+1)-th solution, thus *growing set scheme*. The proposed score calculation is meaningful when the elements in the set are numerous enough.

The whole procedure is repeated up to the convergence. If the method converges, it will identify a single Pareto-optimal solution.

5. OPTIMISATION RESULTS

When optimising a motor design aiming to improve its performance, one of the most challenging tasks is certainly to increase the efficiency η (%). In order to investigate the advantages of multiple-objective optimisation context – both the all-objective and many-objective – over a single-objective context, several runs of various optimisation algorithms have been done. In Table 1, the results of the optimizations are shown. In the second column (2) the values of the five selected design variables (**X**-space) along with five objective functions (**X**-space) for the prototype motor, i.e. the initial values, are shown.

First, the optimal shape design of the studied permanent magnet motor was carried out considering a sequence of single-objective optimizations focused on each objective function separately. For the sake of an example, the results relevant to the minimization of function $f_3(x) = \eta$ are shown in column (3); the efficiency is increased for 3.616%.

However, the mass of active materials m_{tot} is increased for 13.32% in this single-objective optimization. Hence when optimising a motor, it is not recommended to consider only one target quantity (here η), because while maximising a single objective function, other important performance characteristics might be significantly deteriorated.

In contrast, other solutions are found in both all-objective (AO) and many-objective (MO) context, proposed here and described previously. The results are given in columns (4) and (5).

Hereafter features and performance characteristics from AO and MO runs, in comparison with the prototype values (PT) of the PMSM will be analysed; the focus is put on the design variables x_1–x_5 and individual objective functions f_1–f_5, as well as few more features of interest for the permanent magnet motor performance.

Table 1 Optimisation results for PMSM

X-space (unit) \ **F**-space (unit)	Prototype Motor – PT	Maximise efficiency: f_3	ALL Objectives Design – AO	MANY Objectives Design – MO
(1)	(2)	(3)	(4)	(5)
x_1: Rotor radius R_R (mm)	42.2	36.0	35.9	36.57
x_2: Air-gap length g (mm)	0.8	0.8	0.7	0.79
x_3: PM length h_{PM} (mm)	2.0	2.0	2.3	2.29
x_4: PM pole coverage f_m	0.9	0.89	0.82	0.79
x_5: Axial motor length L (mm)	90	103.4	76.5	83.9
f_1: Total loss P_{loss} (W)	186.5	143.3	184.2	177.7
f_2: Total mass m_{tot} (kg)	8.79	9.96	7.73	8.31
f_3: Efficiency η (%)	84.89	87.96	85.04	85.49
f_4: Design factor D^2L*e-04 (m3)	7.29	6.23	4.63	5.28
f_5: Torque density T_n/V_m*e+03 (Nm/m^3)	7.76	9.05	9.13	8.33

In order to obtain comparable results, the elements of **X**-space and **F**-space vectors are normalised accordingly to the respective initial values from the prototype motor, taken as reference. Taking into consideration columns (2), (4) and (5) from Table 1, the graphical presentations for normalised design variables and normalised objective functions are presented in Figure 6 and Figure 7, respectively.

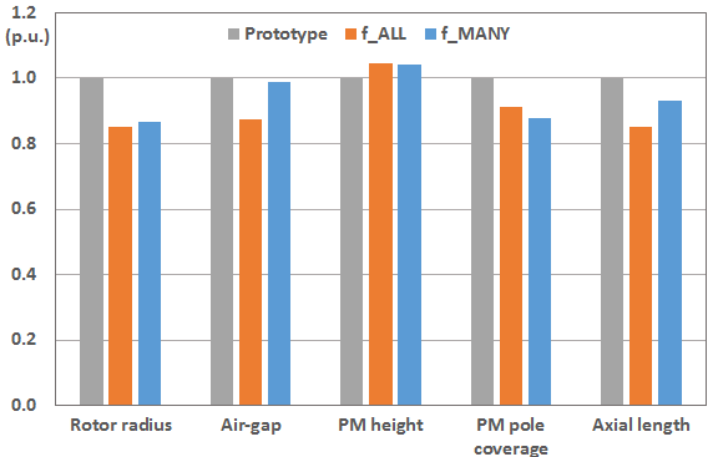

Figure 6: Comparative charts for X-space

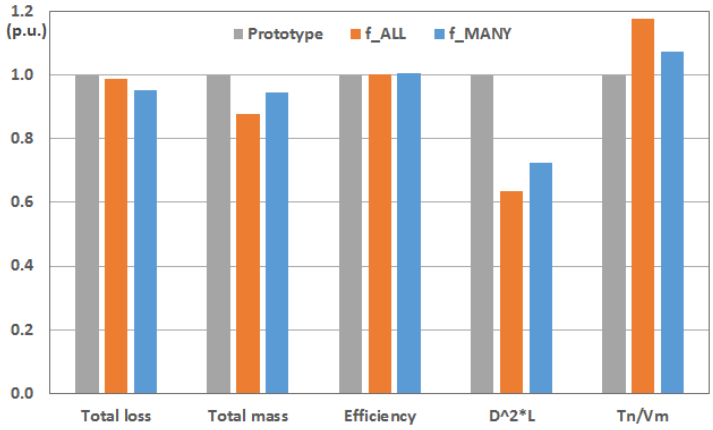

Figure 7: Comparative charts for F-space

To visualise the computed optimal design variables $x_1 - x_5$ for AO and MO design, a combined lamination geometry of the PMSM, connected to the prototype PT motor is presented in Figure 8. It is worth mentioning once again, that outer stator diameter and inner rotor diameter were kept the same as for the reference motor. At first glance, the both optimisation algorithms AO and MO determine similar lamination geometry, also seen in Table 1.

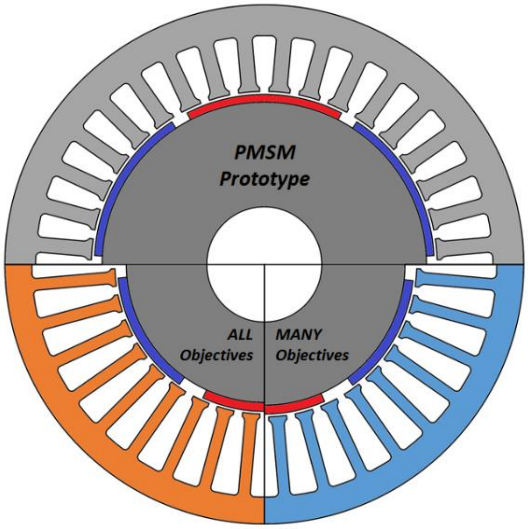

Figure 8: Lamination geometry comparison based on design variables

6. MOTOR PERFORMANCE ANALYSIS

To assess the quality of optimised PMSM models, an investigative study for the quantities f_1-f_2 from **F**-space has been carried out. The motor efficiency is dependent on the total power loss. Hence, an interesting issue to be analysed is distribution of losses, where the copper loss is a dominant component. The results presented in Table 2 are calculated for nominal operating regime of the motor, i.e. at torque T_n = 10 Nm and speed n_n = 1000 rpm. Another quantity of interest is the total mass of active materials, distributed among copper for windings, iron for cores and permanent magnets, as shown in the table below.

Table 2 Loss and mass components

Symbol	Description (unit)	Prototype Motor – PT	ALL Objectives Design – AO	MANY Objectives Design – MO
P_{Fe}	Iron loss (W)	17.4	14.5	14.9
P_{Cu}	Copper loss (W)	147.1	147.7	140.8
P_{fw}	Mechanical loss (W)	22.0	22.0	22.0
P_{tot}	Total loss (W)	186.5	184.2	177.7
η	Efficiency (%)	84.89	85.04	85.49
m_{Cu}	Total copper mass (kg)	1.60	2.53	2.58
m_{Fe}	Total iron mass (kg)	6.83	4.93	5.42
m_{PM}	Total PM mass (kg)	0.36	0.28	0.31
m_{tot}	Total mass of active materials (kg)	8.79	7.74	8.31

Due to lowest total loss, MO optimal design of the PMSM is with the highest efficiency, which is an undoubted advantage. However, the drawback is higher utilisation of copper. It is known from theory that so called *copper motors* exhibit improved efficiency, compared to *iron motors*. It is evident that both MO and AO are copper motors, while the prototype is an iron motor. The proof is also found in Figure 8, where the stator slots of MO and AO are with bigger cross-section for inserting bigger number of coil's turns, meaning *more* copper. Simultaneously, the stator yoke height is decreased, meaning *less* iron. In addition, axial length *L* of the new optimised motors (Table 1), compared to the prototype is also decreased, which enhances the effects.

6.1. Magnetic Field Distribution

The analysis of the magnetic field distribution is used as a matching method to visualise the effects of new design variables on the overall motor performance. The FEM calculations are performed by using FEMM code (Meeker, 2019), in 2D domain of the permanent magnet motor. A combined presentation for the magnetic field distribution in the analysed PMSM designs is given in Figure 9. Evidently, magnetic circuit saturation of the stator yoke is lower in the optimised AO and MO motors that contributes to reduction of the yoke loss. On the other side, because of reduced tooth width, the teeth are higher saturated. But, due to decreased iron mass, this iron loss component will be also reduced. Consequently, this is a desirable circumstance which in turn, will increase the motor efficiency.

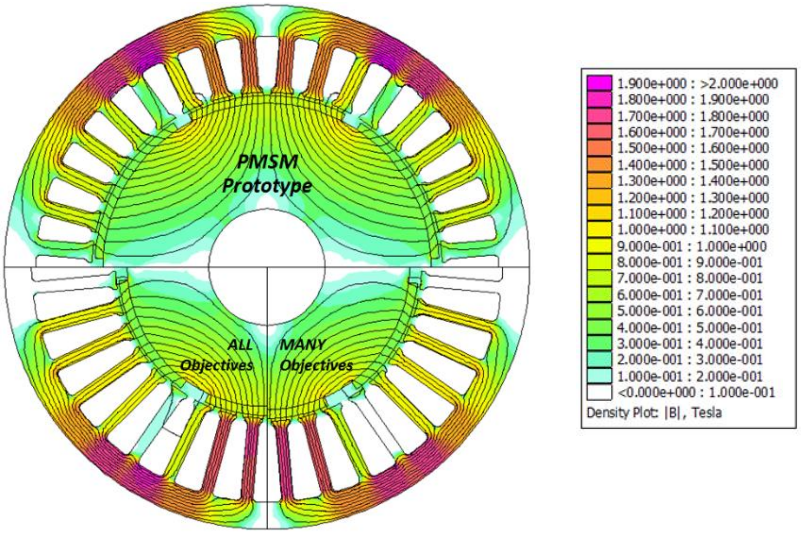

Figure 9: Comparison of magnetic field distribution at no-load

By employing FEA, an extensive electromagnetic performance analysis has been accomplished. The characteristics of interest are air-gap magnetic flux per pole and magnetic flux density distribution along a mid-gap line, spanned over a pole pair pitch. The characteristics are presented in Figure 10 and Figure 11, respectively. The figures show that AO and MO motor model have similar shape of characteristics, with close values. As a conclusion, the previously discussed advantages of the optimal MO design, accompanied with AO design, remain in force without deterioration of the PMSM electromagnetic features.

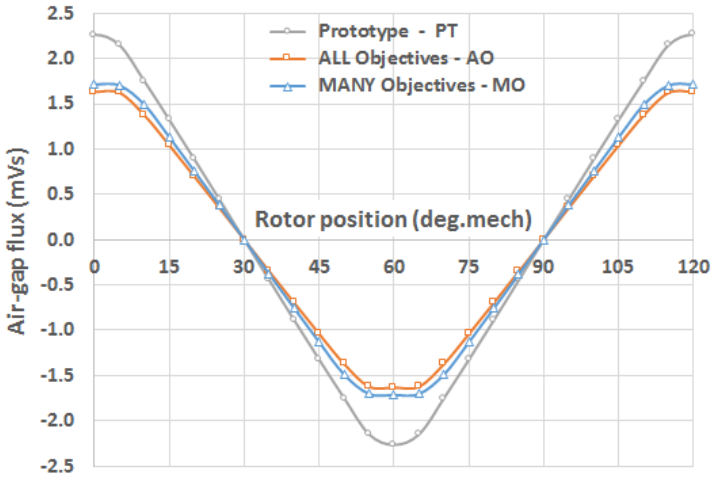

Figure 10: Air-gap magnetic flux per pole vs rotor position

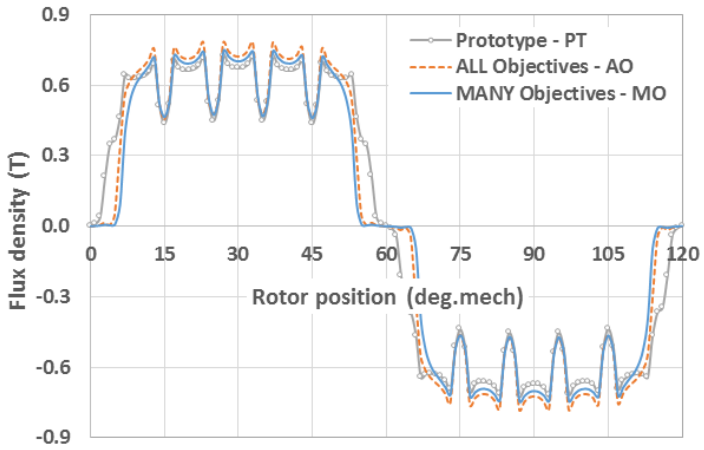

Figure 11: Mid-gap magnetic flux density at no-load along a pole pair pitch

6.2. Torque characteristics

The evaluation of the PMSM torques – cogging and electromagnetic – is carried out on the basis of a comparative presentation of the characteristics. It is started with determination of cogging torque characteristics, a challenging matter for research and analysis of permanent magnet motors (Pang *et al*., 2011). Cogging torque in PMSM comes from variations of the magnetic field density around the edges of the rotor permanent magnets as they pass the non-uniform geometry of the stator, due to the presence of slots. Thus cogging torque is produced by the tendency of the rotor to align with the stator, at positions where the permeance of the magnetic circuit is maximised (Petkovska *et al*., 2011). Calculations for the three designed PMSM motors are carried out for one full period of the cogging torque change, i.e. for one stator tooth pitch equal to 10^0 mech.

The comparative characteristics are presented in Figure 12. The different sign in the prototype motor model PT, compared to AO and MO optimised motor models is evident. The explanation for this phenomenon is found in the value of air-gap permeance. Namely, there is a tendency rotor to move toward the position where it is higher, which determines the direction of the rotation, and consequently the cogging torque sign. However, it is worth to emphasise that only the peak-value, but not sign of cogging torque has an effect on the motor performance.

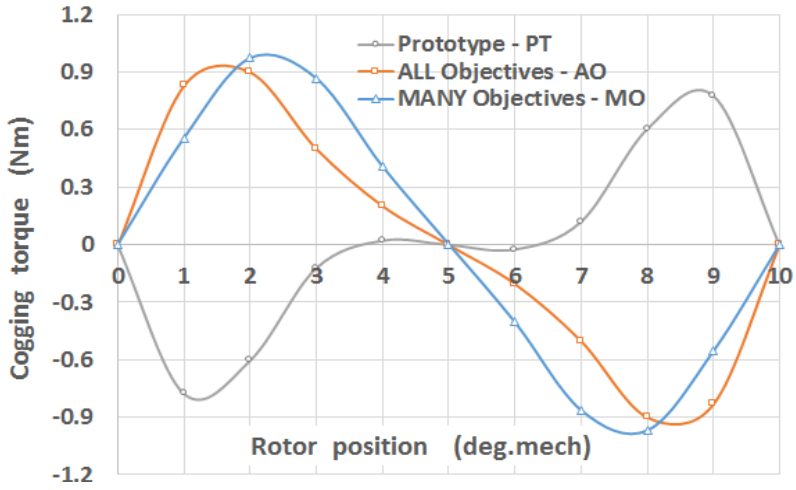

Figure 12: Comparison of cogging torque profiles

An investigation of the cogging torque characteristics shows increased peak-value in the both optimal motor designs together with polarity change. The explanation is found in the stator slot opening dimension, which should keep the value of the prototype; this technical requirement is necessary for easy inserting the stator windings coils. As seen in Figure 8, the radius of stator bore in PT motor is biggest, providing better ratio for tooth tip arc over slot opening and thus, the lowest cogging peak. On the other hand, AO and MO designs have smaller inner stator radiuses, but in favour of AO. Because of that the AO design is with slightly lower peak. Another difference, as discussed before, is change of the polarity, which in turns ensures higher values for electromagnetic torque at initial rotor positions, meaning more reliable and stable motor starting.

The analysis of static torque characteristics is the next task. For precise electromagnetic torque calculations, by using FEM, accurate global and local field solutions are required. In other words, a high level of mesh discretisation is a prerequisite (Ionel *et al.*, 2005). The preferred method for calculating the electromagnetic torque is by using the weighted stress tensor of a volume integral in the air-gap domain. The rated load was simulated by a respective rated phase current for each motor model, while the rotor is enabled to freely rotate in CW direction (Petkovska *et al.*, 2011). The solution problem is 2D magnetostatic and is performed for one full period, meaning a span over 120 degrees mechanical. The comparative electromagnetic torque characteristics vs rotor displacement are presented in Figure 16. The higher maximum torque values for AO and MO, compared to PT is apparent, where the many objectives MO optimal motor design exhibits the highest values. Also, their steeper curves provide more stable motor operation under load variations. Furthermore, the new optimal design appear to produce similar torque as the prototype design. The next task to be studied is to investigate the measures to undertake, Petkovska *et al.* (2020), in order to mitigate the obviously higher torque pulsations in AO and MO, certainly an undesirable phenomenon.

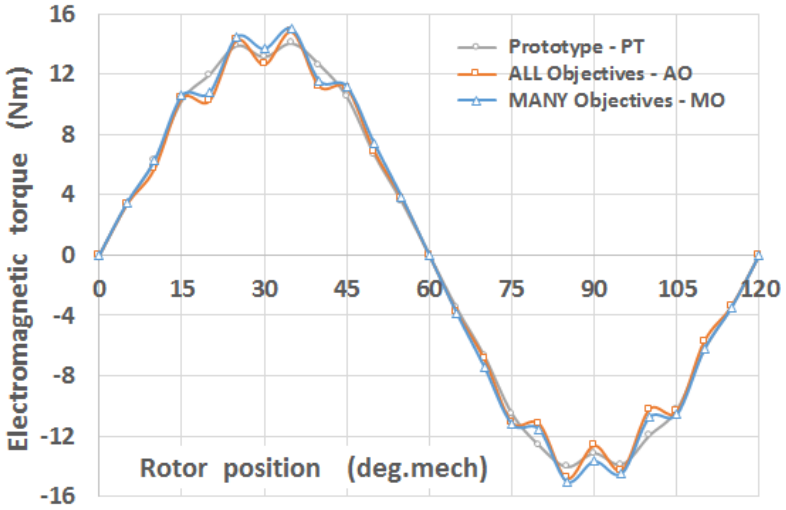

Figure 13: Electromagnetic torque vs rotor position angle

7. CONCLUSION

Finding an electric motor optimal shape design that will satisfy the given requirements can be an overwhelming task due to large number of parameters whose effects on design quality and motor performance are strongly coupled. The paper deals with optimal shape design by minimizing multiple objective functions according to an original interpretation of Pareto optimality. The all-objectives and many-objectives optimization techniques, for a class of PMSM motors are elaborated and performed. An evolution strategy method is applied for the minimization of a weight-free preference function. In the class of evolutionary algorithms, the Evolution Strategy of the zero order (EStra) is an algorithm of single-objective optimization.

The optimisation results, for the **X**-space and **F**-space in all-objectives and many-objectives context, applied for shape design of a permanent magnet synchronous motor (PMSM) are compared to the prototype motor and analysed and discussed. By using FEM the magnetic field distribution in the three motor models is computed. Characteristics relevant for the motor performance evaluation are calculated and presented comparatively on charts. By using prototype performance characteristics as reference, the assessment of the achievements from the both optimisation approaches is presented. The two optimised designs AO and MO show higher efficiency and improved performance parameters and characteristics, with an advantage of the motor shape design obtained by many-objective optimisation technique.

References

Cvetkovski G. V., Petkovska L., (2021), "Selected Nature-Inspired Algorithms in Function of PM Synchronous Motor Cogging Torque Minimisation", PED Journal – *Power Electronics and Drives*, Vol. 6 (41), pp.204-217, https://doi.org/10.2478/pead-2021-0012.

Di Barba P., Mognaschi M.E., Rezaei N., Lowther D.A., Rahman T., (2019), "Many-objective shape optimisation of IPM motors for electric vehicle traction", *International Journal of Applied Electromagnetics and Mechanics*, 60 (S1), pp. S149-S162.

Di Barba P., Mognaschi M. E., (2005), "Recent experiences of multiobjective optimisation in electromagnetics: A comparison of methods," *COMPEL*, Vol. 24, No. 3, pp. 921–930, doi: 10.1108/03321640510598238.

Di Barba P., Mognaschi M. E., (2009), "Industrial Design With Multiple Criteria: Shape Optimization of a Permanent-Magnet Generator," *IEEE Transaction on Magnetics*, Vol. 45, No. 3, pp. 1482–1485, doi: 10.1109/TMAG.2009.2012685.

Di Barba P., Mognaschi M.E., Wiak S., (2020), "A non-differential method for solving many-objective optimization problems: An application in IPM motor design", *International Journal of Applied Electromagnetics and Mechanics*, 64 (S1), pp. S131-S142.

Ionel D. M., Popescu M., McGilp M. I., Miller T. J. E., Dellinger S. J., (2005), "Assessment of Torque Components in Brushless Permanent-Magnet Machines through Numerical Analysis of the Electromagnetic Field", *IEEE Transactions on Industry Application*, Vol. 41, No. 5, pp. 1149–1158. DOI: 10.1109/TIA. 2005.853377.

Jabbari A., Shakeri M., Nabavi-Niaki S. A., (2010), "Pole Shape Optimization of Permanent Magnet Synchronous Motors Using Reduced Basis Technique", *Iranian Journal of Electrical&Electronic Engineering*, Vol.6, No.1, pp. 48-55.

Meeker D., "FEMM – Finite Element Method Magnetics", Software Version 4.2 (2019), https://www.femm.info/wiki/HomePage.

Najgebauer M., Szczyglowski J., Slusarek B., Przybylski M., (2019), "Scaling algorithms in modelling of power loss in soft magnetic composites", COMPEL – *The International Journal for Computation and Mathematics in Electrical and Electronic Engineering*, Vol. 38, No. 4, pp. 1064-1074.

Pang Y., Zhu Z. Q., Feng Z. J., (2011), "Cogging Torque in Cost-Effective Surface-Mounted Permanent-Magnet Machines", *IEEE Transactions on Magnetics*, Vol. 47, No. 9, pp. 2269-2276.

Pellegrino G., Jahns Th.M., Bianchi N., Soong, W., Cupertino, F., (2016), "*The Rediscovery of Synchronous Reluctance and Ferrite Permanent Magnet Motors*". Springer International Publishing, Series SpringerBriefs in Electrical and Computer Engineering, Springer Nature (also Springer-Verlag) AG, Cham Switzerland, eBook ISBN 978-3-319-32202-5, pp. VIII, 136, DOI 10.1007/978-3-319-32202-5_1.

Petkovska L. Cvetkovski G., (2011), "Assessment of Torques for a Permanent Magnet Brushless DC Motor Using FEA, *Przeglad Elektrotechniczny*, Vol. 87, No. 12b, pp. 132-136.

Petkovska L., Lefley P., Cvetkovski G., (2012), "Synthesis and Analysis of a High-Performance Low-Cost Permanent Magnet Brushless DC Motor", COMPEL – *The International Journal for Computation and Mathematics in Electrical and Electronic Engineering*, Vol. 31, No.5, pp. 1482-1491.

Petkovska L., Lefley P., Cvetkovski G. V., (2020), "Design Techniques for Cogging Torque Reduction in a Fractional-Slot PMBLDC Motor£, COMPEL – *The international journal for computation and mathematics in electrical and electronic engineering*, Vol. 39, No. 5, pp. 1041-1055.

Przybylski M., Ślusarek B., Di Barba P., Mognaschi M. E., Wiak S., (2020), "Temperature and torque measurements of switched reluctance actuator with composite or laminated magnetic cores", *MDPI Journal Sensors* (Basel, Switzerland), Vol. 20, 3065, pp. 1-14, https://doi.org/10.3390/s20113065.

Putek, P., Paplicki, P., Pulch, R., Ter Maten, E.J.W., Günther, M., Pałka, R., (2017), "Multi-objective topology optimization of a permanent magnet machine to reduce electromagnetic losses and cogging torque", *International Journal of Applied Electromagnetics and Mechanics*, 53 (S2), pp. 1-10.

Villani M., (2018), "High Performance Electrical Motors for Automotive Applications – Status and Future of Motors with Low Cost Permanent Magnets", *Proceedings of the 8th International Conference Magnetism and Metallurgy – WMM'18*, pp. 1-15, Dresden, Germany.

Yan, W., Chen, H., Liu, X., Ma, X., Lv, Z., Wang, X., Palka, R., Chen, L., Wang, K., (2019), "Design and multi-objective optimisation of switched reluctance machine with iron loss, *IET Electric Power Applications*, 13 (4), pp. 435-444.

Zhang B., Andreas S., Doppelbauer M., (2016), "Development of a Novel Yokeless and Segmented Armature Axial Flux Machine Based On Soft Magnetic Powder Composites", In the *World PM2016 Proceedings USB*. Published by EPMA – European Powder Metallurgy Association, https://www.worldpm2016.com/. Technical paper presented at World PM2016 Congress & Exhibition, Hamburg, Germany.